

TECH. MEMO  
M&S 1126

UNLIMITED

BR110495

TECH. MEMO  
M&S 1126

②

616 FILE 1021



ROYAL AEROSPACE ESTABLISHMENT

AD-A210 958

CALIBRATION OF A PULSED POTENTIAL CRACK  
MONITOR FOR USE IN FATIGUE CRACK GROWTH STUDIES

by

J. Newman  
A. Jefferson  
P.J. Gregson  
P.D. Pitcher

April 1989

DTIC  
ELECTE  
AUG 08 1989  
S E D

Procurement Executive, Ministry of Defence  
Farnborough, Hants

UNLIMITED

89 8 08 113

UNLIMITED

ROYAL AEROSPACE ESTABLISHMENT

Technical Memorandum M&S 1126

Received for printing 11 April 1989

CALIBRATION OF A PULSED POTENTIAL CRACK  
MONITOR FOR USE IN FATIGUE CRACK GROWTH STUDIES

by

J. Newman\*

A. Jefferson\*\*

P.J. Gregson\*

P.D. Pitcher

SUMMARY

→ A pulsed direct current is used to generate a potential drop as a function of crack length. Experimental values of potential drop and crack length have been obtained for three test-piece geometries: a centre crack specimen, a holed specimen (AGARD), and a compact tension specimen. Computed values have been generated using a Fortran program and are compared with the experimental results. Comments are made on the accuracy of the technique and its consequences on potential probe positioning for both short and long cracks. Great Britain (AU)

Copyright

©

Controller HMSO London  
1989

---

\* Engineering Materials, Southampton University, Southampton, SO9 5NH  
\*\* Department of Aeronautics and Astronautics, Southampton University, Southampton SO9 5NH

UNLIMITED

1

LIST OF CONTENTS

	<u>Page</u>
1 INTRODUCTION	3
2 EXPERIMENTAL PROCEDURE	3
3 RESULTS	4
3.1 Centre cracked specimen (CCS)	4
3.2 AGARD specimen	4
3.3 Compact tension specimen (CTS)	5
4 DISCUSSION	5
5 CONCLUSIONS	6
Acknowledgment	6
References	7
Illustrations	Figures 1-11
Report documentation page	inside back cover

Accession For	
NTIS GR&I	<input checked="" type="checkbox"/>
DTIC TAB	<input type="checkbox"/>
Unannounced	<input type="checkbox"/>
Justification	
By _____	
Distribution/	
Availability Codes	
Avail and/or	
Dist	Special
A-1	



## 1 INTRODUCTION

Accurate measurement of crack length is a necessary criterion for detailed analysis of the fatigue (or fracture toughness) performance of a material.

Several methods exist but one of the most versatile uses the phenomenon of potential drop. When a constant direct current supply is applied to a cracked specimen, a potential can be measured across a crack. This potential is a function of specimen geometry and crack length. In developing this simple principle, Sutton<sup>1</sup> employed a pulsed current to reduce errors from supply frequency pick-up, thermoelectric emf and the effects of crack closure; furthermore two pairs of probes were used to give a voltage ratio which was independent of current variation and temperature.

Sutton<sup>1</sup> and Eastabrook *et al*<sup>2</sup> conducted their initial experimental calibrations of the pulsed pd system on large mock-ups of their specimen geometries using thin aluminium foil. This was then cut to model the extending crack, and also elastic and plastic deformation of loaded test specimens<sup>2</sup>. McCartney *et al*<sup>3</sup> compared theoretical values of potential drop against crack length with experimental values. The theoretical values of potential ratio were obtained from Laplace equations and were found to be in good agreement with measured values. Ingelbrecht and Ward-Close<sup>4</sup> also found good agreement when they used NAG routines based on McCartney *et al*'s<sup>3</sup> Laplace solutions. Over-estimates of the potential at short crack lengths were noted and the authors concluded that specimen geometry and accurate probe positioning close to the crack were of importance.

This system has subsequently been developed commercially and this Memorandum sets out to describe the calibration of such a crack monitor for several test piece geometries which are used by engineers in the study of fatigue crack growth behaviour.

## 2 EXPERIMENTAL PROCEDURE

In the present work the calibration of three fatigue specimen geometries was undertaken:

- (i) centre-crack specimen (CCS) - Fig 1
- (ii) unloaded holed AGARD specimen (AJARD) - Fig 2
- (iii) compact tension specimen (CTS) - Fig 3.

All the specimens were prepared from 0.6mm aluminium foil; specimen dimensions are given in the figures.

The crack length was monitored via a Howdens potential drop system operating with a pulsed directed current of 10A peak. For the CTS foil the current was applied as a point source whilst for the CCS and AGARD foils the current was applied uniformly across the foil by attaching fish-plates to the foil. The electrical potential produced was measured by two pairs of electrode probes: the 'inner probes' ( $P_1$ ) and the 'outer probes' ( $P_2$ ) - see Figs 1 to 3.

For each crack increment (5 mm for the CCS and AGARD foils and 10 mm for the CTS foil) the potentials  $P_1$  and  $P_2$  were measured and hence the voltage ratio ( $P_r = P_1/P_2$ ) was obtained for various  $a/W$  values (where  $a$  = crack length and  $W$  = specimen width). For the CCS foil the inner probe position ( $P_1$ ) was kept constant at 4 mm from the crack front with the outer probe position ( $P_2$ ) varying from 55 to 95 mm. The AGARD specimen had varying  $P_1$  and  $P_2$  with  $P_1$  measured from 21.8 to 46.8 mm and  $P_2$  55 to 95 mm away from the central axis of the sheet. The CTS foil also had varying  $P_1$  and  $P_2$  probe positions - see Fig 3.

Ingelbrecht and Ward-Close<sup>4</sup> wrote a Fortran computer program that used NAG routines to generate calibration tables of crack length-electrical potential. A similar program was developed to compute calibration tables for the three test-piece geometries used in the present work.

### 3 RESULTS

#### 3.1 Centre cracked specimen (CCS)

The results of the experimental calibration for the centre crack specimen are shown in Fig 4 for three positions of the outer probe ( $P_2$ ). The curves are very similar to those of Sutton<sup>1</sup> although the actual positions of the probes were not exactly the same. Fig 5 compares the experimental results for  $P_1 = 4$  mm and  $P_2 = 75$  mm with the computed values for the same probe positions. A good agreement is seen between the results for almost all the  $a/W$  range although there is some discrepancy when  $a/W$  is greater than about 0.85.

#### 3.2 AGARD specimen

Similar data to that of the CCS foil were obtained for the AGARD specimen; voltage ratios for selected combinations of  $P_1$  and  $P_2$  are included in Fig 6. For each inner probe position ( $P_1$ ) curves were plotted for the range of  $P_2$  values similar to Fig 4 for the CCS foil. It can be seen that as  $P_1$  is moved further from the crack front the potential ratio against  $a/W$  curves becomes less steep and hence less sensitive to voltage change for a given increment in crack length; additionally the curves become more widely space. The experimental results and computer predictions of the potential ratio- $a/W$  curves for  $P_2 = 80$

and 95 mm are shown in Figs 7 and 8 for inner probe positions  $P_1 = 21.8$  and 26.8 mm respectively. It should be noted that for the computer predictions the hole was represented by 24 chord elements in order that the geometry had linear boundaries, but the agreement between predicted and experimental results is good. However, discrepancy occurs when  $a/W$  values are high.

### 3.3 Compact tension specimen (CTS)

Results for the CTS foil are shown in Figs 9 and 10 for two  $P_1$  and  $P_2$  positions. It can be seen that there is very good agreement between predicted and experimental values for all probe positions.

## 4 DISCUSSION

The accurate measurement of crack length during fatigue tests is essential to designers in their attempts to derive conservative estimates of fatigue life using fracture mechanics. The use of the potential drop technique for measuring crack length is well documented (*eg* Refs 1 to 5) and is proven to be an acceptable method.

The results of the CCS geometry presented here serve two purposes: confirmation of the accuracy and efficiency of the experimental technique and the reproducibility of the results (*cf* those of Sutton<sup>1</sup> for a similar geometry). In addition the close agreement found between the experimental values and those provided by the computer program of Ingelbrecht and Ward-Close<sup>4</sup> allow more thorough consideration of the other two geometries.

For the AGARD specimen it was initially thought that the presence of a comparatively large hole (*ie* its diameter was a quarter of the total width) would cause some variation in current contours within the specimen; these effects may influence the potential readings and thus reduce the sensitivity of crack length measurement. However, it was found that the experimental results and the computed values for short cracks were largely unaffected by the hole. At long crack lengths the potential readings showed fluctuation and instability when  $P_1$  was high (greater than 36.8 mm) and  $P_2$  low (less than 70 mm). Therefore the inner probes ( $P_1$ ) should be located close to the hole and the outer probes ( $P_2$ ) distant from the hole whilst not being influenced by the current input. The series of curves produced for the various  $P_1$  and  $P_2$  probe positions showed a decrease in the slope of the curves as  $P_1$  increased. Since the gradient of these curves provides an indication of the sensitivity, it follows that the greatest accuracy would be obtained by using low  $P_1$  values and high  $P_2$  values. This is borne out by the good agreement between the experimental and computed values plotted

in Figs 7 and 8. The slight discrepancy between experimental and computed results at high  $a/W$  ratios would be of importance to workers interested in propagation at long crack lengths. For fatigue crack growth testing, it may be necessary to compromise between optimum sensitivity of crack length measurements and practicalities of probe positioning and attachment.

The results for the CTS foil show good agreement between the computed and experimental values for all the probe positions - see Figs 9 and 10. The similar slopes in these graphs shows that for the CTS geometry sensitivity is unaffected by probe positioning.

Ingelbrecht and Ward-Close<sup>4</sup> produced a potential ratio against crack length curve using their computer program for a compact tension specimen and this has been replotted in Fig 11 where a comparison is made with the present results. The potential values for the Ingelbrecht and Ward-Close specimen are higher, the offset is similar for increasing  $a/W$  values with the gradient of both curves being approximately the same. The curves have a similar shape and the difference in potential values can be accounted for by the difference in specimen geometries, and, to some extent the probe ( $P_1$ ) positions. The agreement between the results of the present study and those of Ingelbrecht and Ward-Close provides evidence of reproducibility and accuracy of the present experimental technique.

## 5 CONCLUSIONS

- (1) The experimental system produces a useful calibration of potential drop against crack length for three test-piece geometries: a centre crack specimen, a holed specimen (AGARD), and a compact tension specimen.
- (2) The experimental results show a good agreement with computed values and also compare favourably to previously published data.
- (3) The positioning of the potential probes can be of importance, particularly for the centre crack and AGARD specimens. Varying probe position can affect the sensitivity of the measurement technique which may have some influence on the accuracy of crack length determination.
- (4) Actual positioning of potential wires to match the optimum positions selected from the calibration may not always be possible and hence a compromise for accuracy of crack length measurement and ease of positioning may occur.

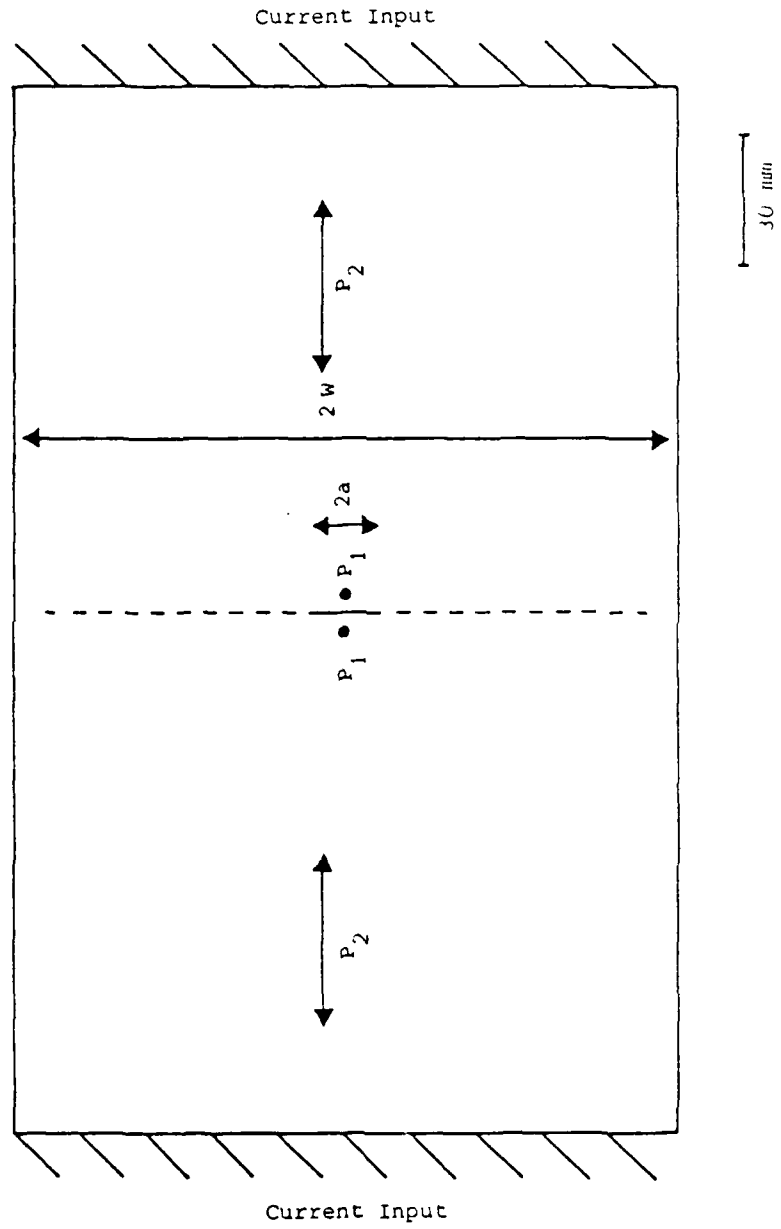
## Acknowledgment

The financial support from MoD(PE) and British Aerospace is gratefully acknowledged. The work was carried out as part of Research Agreement 2040/411/XR MAT.

REFERENCES

- | <u>No.</u> | <u>Author</u>                                | <u>Title, etc</u>   |
|------------|--|---|
| 1          | G.R. Sutton                                  | An improved electrical potential method for crack length measurement.<br>Technical Report 83063, RAE, Farnborough, UK (1983)  |
| 2          | J.N. Eastabrook<br>C. Wheeler<br>G.R. Sutton | Electrical measurement of crack length in loaded specimens.<br>Technical Report 84086, RAE, Farnborough, UK (1984)  |
| 3          | L.N. McCartney<br><i>et al</i>               | Measurement of crack lengths in compact tension and single edge notch specimens using a new electrical potential calibration.<br>NPL, DMA(B)3, February (1977)      |
| 4          | C.D. Ingelbrecht<br>C.M. Ward-Close          | A computer program for the calibration of the dc potential drop method of crack length measurement.<br>Technical Memorandum 392, RAE, Farnborough, UK (1982)        |
| 5          | D.M. Gilbey<br>S. Pearson                    | Measurement of the length of a central or edge crack in a sheet of metal by an electrical resistance method.<br>Technical Report 66402, RAE, Farnborough, UK (1966) |

Fig 1



TM M&S 1126

Fig 1 Schematic diagram of the centre crack specimen foil showing the current input and probe positions.

Fig 2

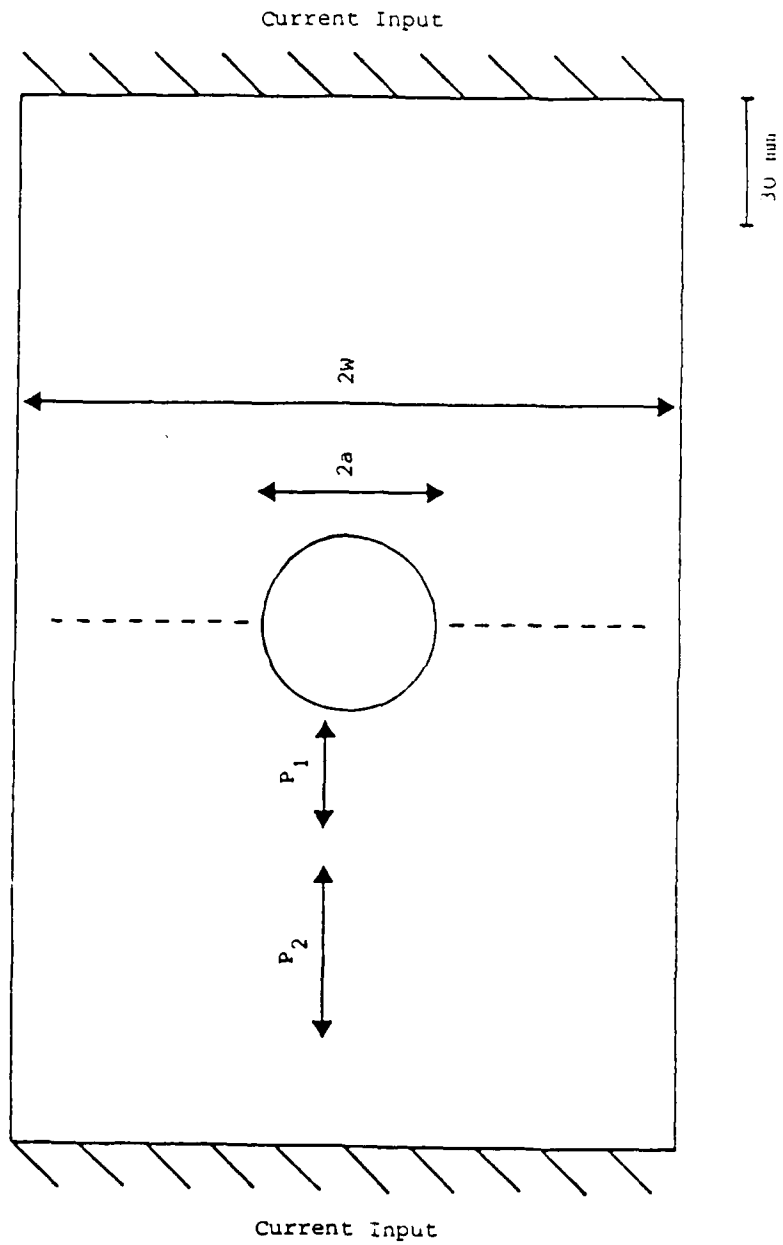


Fig 2 Schematic diagram of the AGARD foil showing the current input and probe positions.

Fig 3

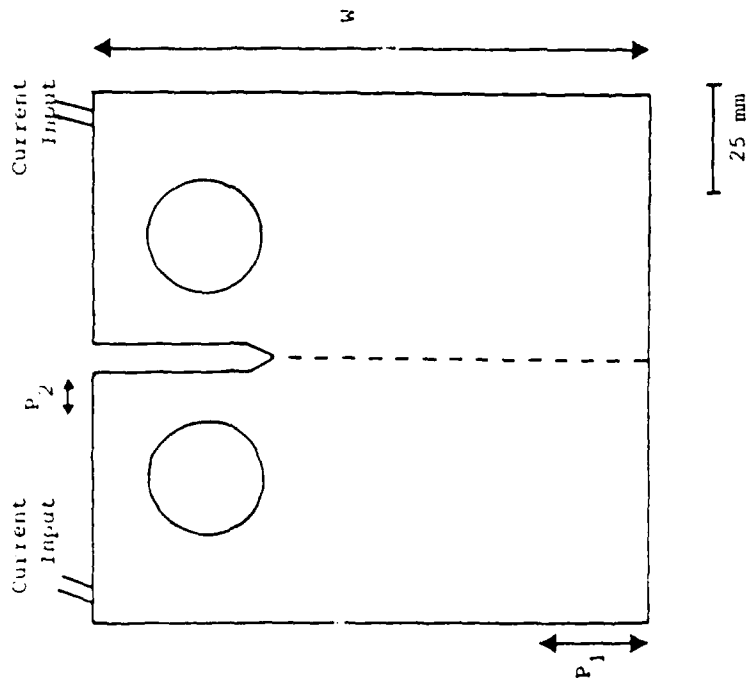


Fig 3 Schematic diagram of the compact tension specimen foil showing the current input and probe positions.

Fig 4

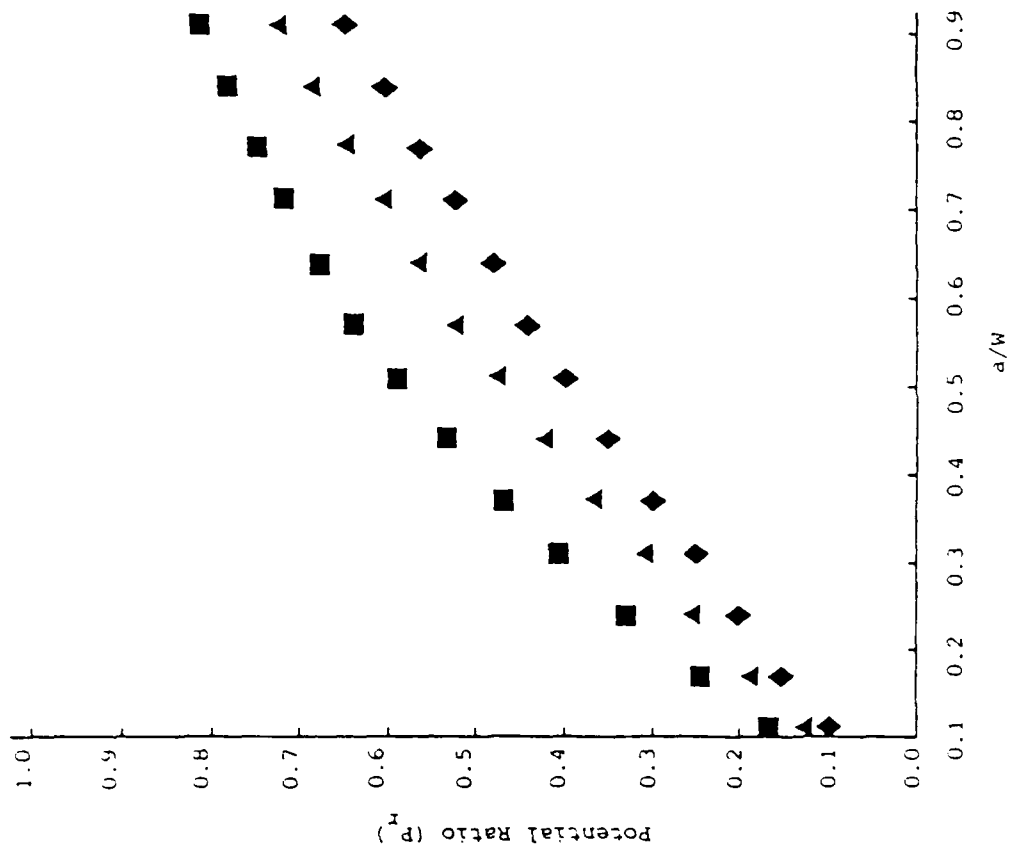
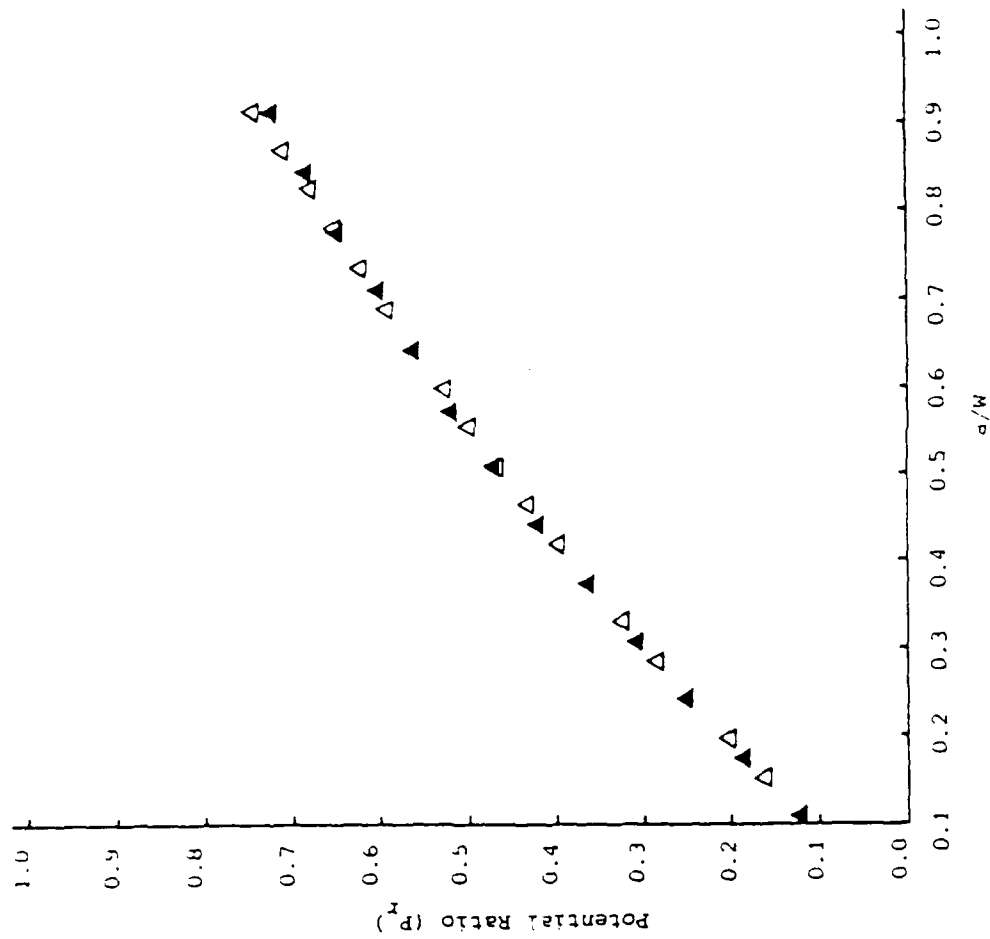


Fig 4 Potential ratio against  $a/W$  for the CCS foil showing the effect of varying the outer probe position ( $P_2$ ).  
■:  $P_2 = 55$  mm; ▲:  $P_2 = 75$  mm; ◆:  $P_2 = 95$  mm

Fig 5



TN M&S 1126

Fig 5 Potential ratio against a/W for the CCS foil for P<sub>1</sub> = 4 mm and P<sub>2</sub> = 75 mm.  
▲ = experimental values; △ = computed values.

Fig 6

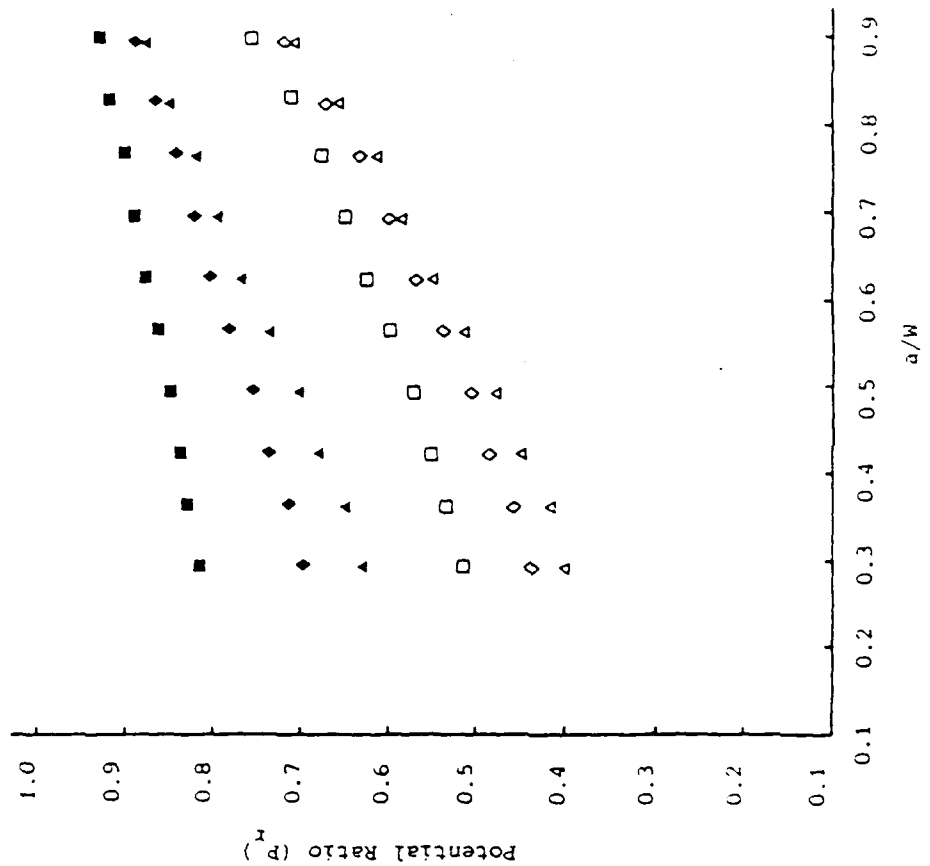


Fig 6 Potential ratio against  $a/W$  for the AGARD foil for varying  $P_1$  and  $P_2$  positions. (Open symbols are for  $P_2 = 95$  mm, closed symbols are for  $P_2 = 55$  mm).  $\triangle \blacktriangle = P_1 = 21.6$  mm;  $\diamond \blacklozenge : P_1 = 31.6$  mm;  $\square \blacksquare : P_1 = 41.6$  mm.

Fig 7

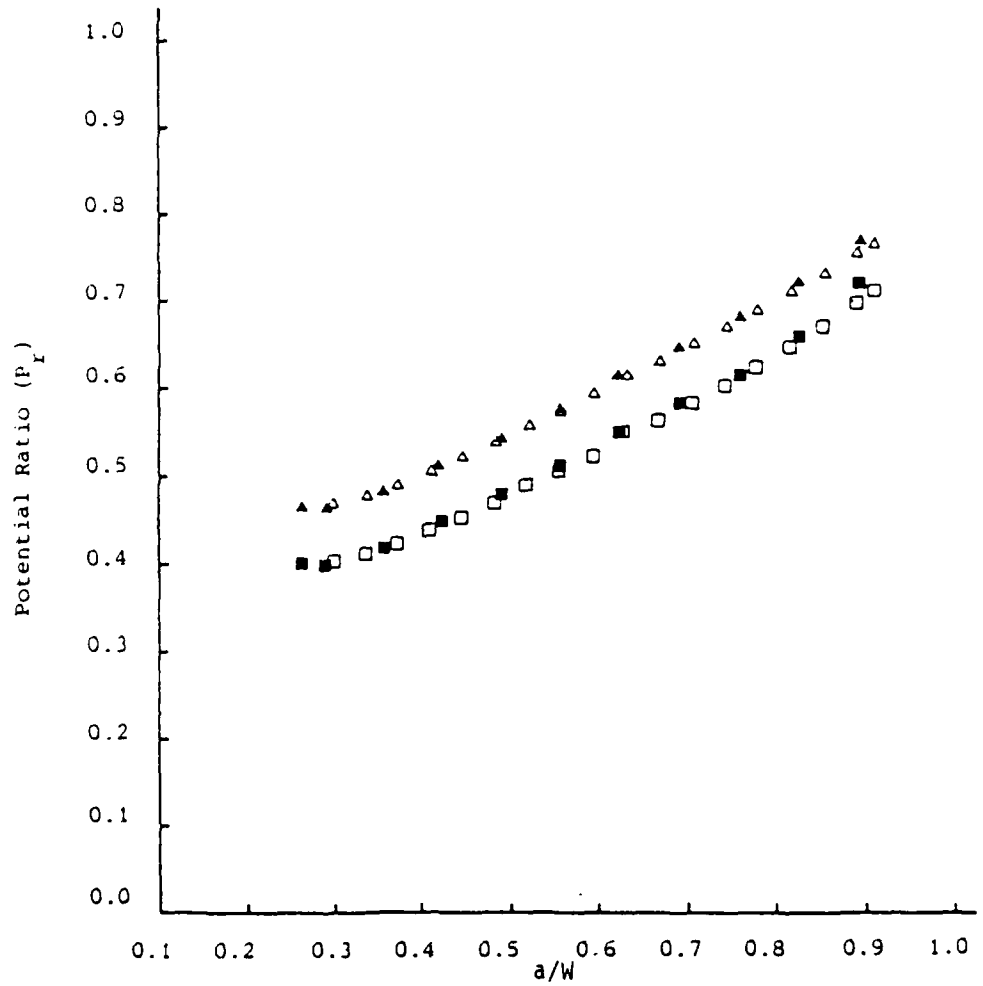


Fig 7 Potential ratio against  $a/W$  for the AGARD foil for computed (open symbols) and experimental values (closed symbols) for  $P_1 = 21.8$  mm;  $\Delta$   $\blacktriangle$ :  $P_2 = 80$  mm  
 $\square$   $\blacksquare$ :  $P_2 = 95$  mm.

Fig 8

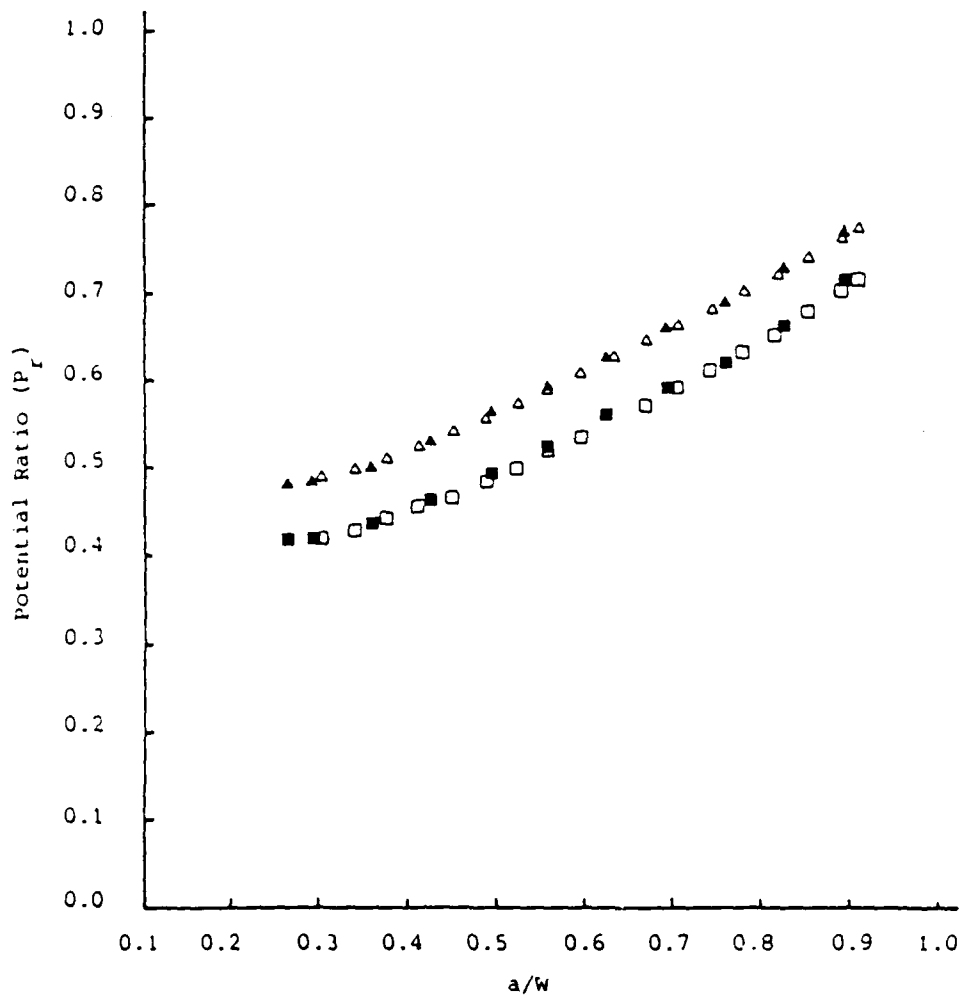


Fig 8 Potential ratio against  $a/W$  for the AGARD foil for computed (open symbols) and experimental values (closed symbols) for  $P_1 = 26.8$  mm,  
 $\triangle \blacktriangle$ :  $P_2 = 80$  mm;  $\square \blacksquare$ :  $P_2 = 95$  mm.

Fig 9

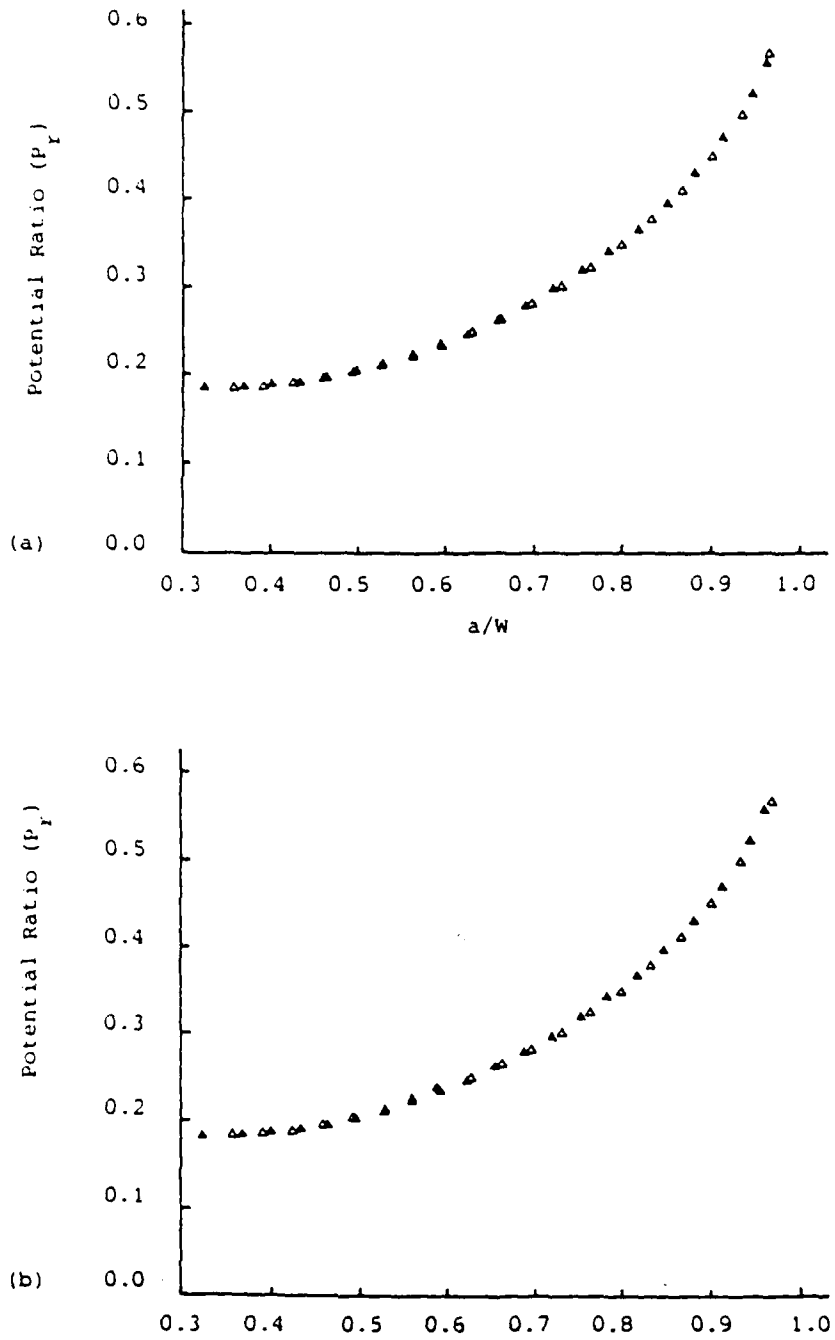


Fig 9 Potential ratio against  $a/W$  for the CTS foil for computed (open symbols) and experimental values (closed symbols) (a)  $P_1 = 0.0$  mm,  $P_2 = 274.25$  mm and (b)  $P_1 = 0.0$  mm,  $P_2 = 264.25$  mm.

Fig 10

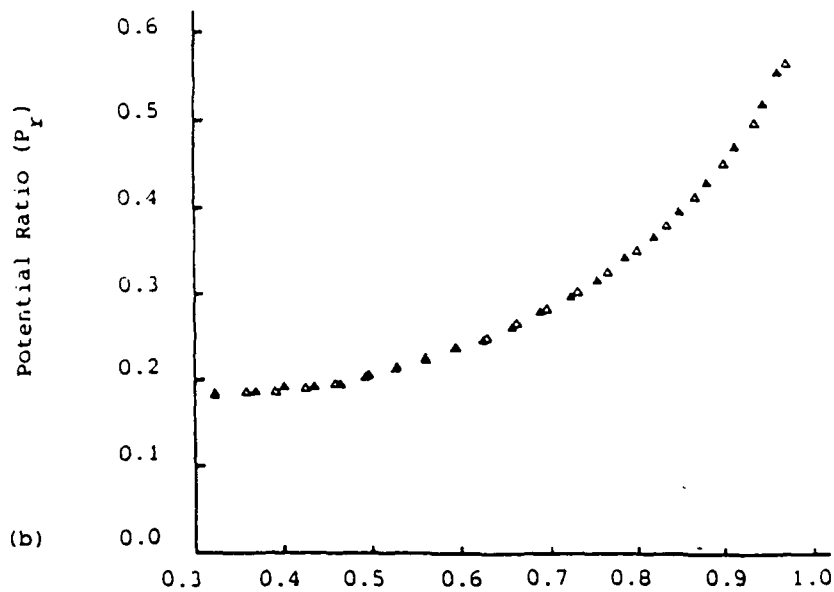
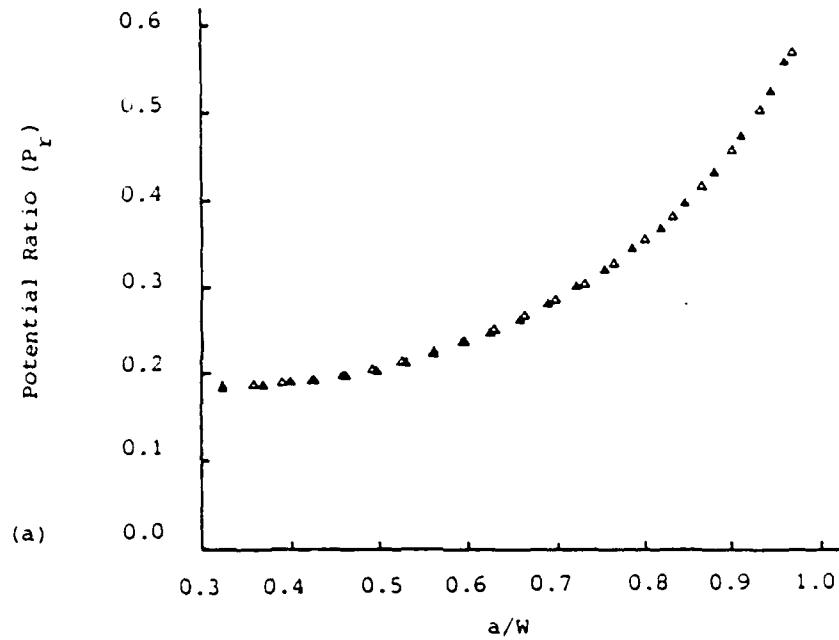


Fig 10 Potential ratio against  $a/W$  for the CTS foil for computed (open symbols) and experimental values (closed symbols) (a)  $P_1 = 25.0$  mm and  $P_2 = 274.25$  mm, and (b)  $P_1 = 25.0$  mm,  $P_2 = 264.25$  mm.

Fig 11

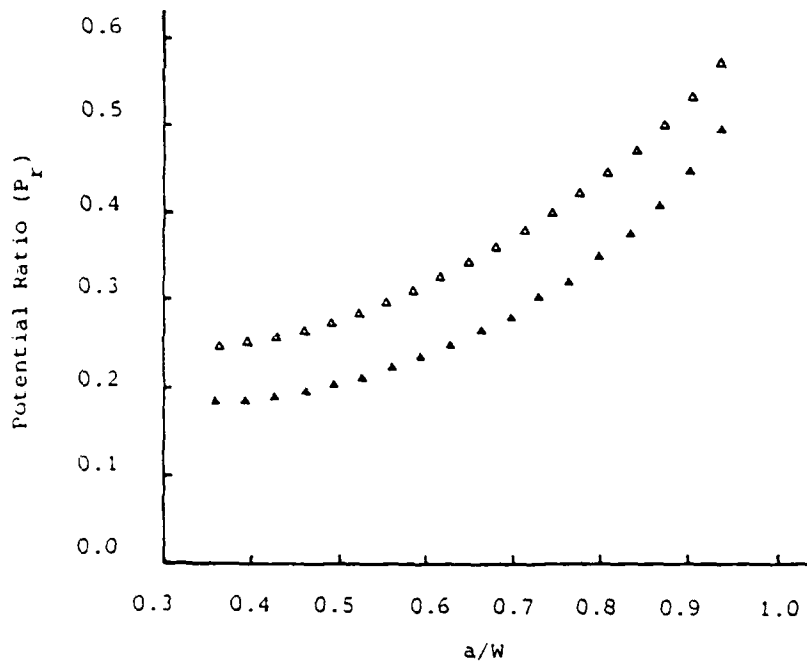


Fig 11 Potential ratio against  $a/W$  for the CTS foil.  $\triangle$  = results from Ingelbrecht and Ward-Close<sup>4</sup>;  $\blacktriangle$  = results from present work for  $P_2 = 0.0$  mm and  $P_2 = 274.25$  mm.

0043244

CONDITIONS OF RELEASE

BR-110495

\*\*\*\*\*

U

COPYRIGHT (c)  
1988  
CONTROLLER  
HMSO LONDON

\*\*\*\*\*

Y

Reports quoted are not necessarily available to members of the public or to commercial organisations.